Peristaltic Flow of Non-Newtonian Fluids through Curved Channels: a Numerical Study

Alireza Kalantari[1], Kayvan Sadeghy[1], and Soheil Sadeqi[2]

[1] School of Mechanical Engineering, College of Engineering, University of Tehran
Center of Excellence for the Design and Optimization of Energy Systems (CEDOES)
P.O. Box: 11155-4563, Tehran, Iran

[2] Mechatronic Systems Engineering, School of Engineering Science
Simon Fraser University, Surrey, BC, Canada

ABSTRACT

Peristaltic flow of a viscoelastic fluid which obeys Phan-Thien-Tanner (PTT) model as its constitutive equation is numerically studied in a curved channel. The flow is assumed to be incompressible, laminar, and two-dimensional. Numerical results show that the elastic behavior of a fluid can significantly decrease the pressure rise of peristaltic pumps for a given flow rate. On the other hand, a radially-imposed magnetic field is shown to increase the pressure rise of the pump when the flow rate is less than a certain value. The results are interpreted in terms of the extensional-flow behavior of the fluid as represented by the fluid's extensional parameter.

INTRODUCTION

A wave propagating along the flexible walls of a channel can induce flow without any need for external pressure gradient. Such flows, which are referred to as peristaltic flows, are encountered in several parts of human bodies including urinary system, chime transport in gastrointestinal tract, reproductive tracts, and female fallopian tube, among others[1,2]. For reasons like these, this particular flow has been the subject of many studies in the past[1,2]. Both Newtonian and non-Newtonian fluids have been addressed in these studies. The interest in non-Newtonian fluids arises from the fact that most physiological fluids behave as non-Newtonian fluids. A variety of rheological models have been used to represent such fluids in the past[3-9]. One can mention, for example, inelastic fluid models such as power-law model, and viscoelastic fluid models such as ordered models, Maxwell model, Oldroyd-B model, and Johnson-Segalman model. Through such studies, the effects of different rheological parameters have been investigated on the performance of peristaltic pumping[3-9].

The rheological models used in previous studies suffer from the drawback that they are poor when it comes to flows dominated by extensional deformations. Peristaltic flows involve a series of propagating converging-diverging flows, and so they are typical of extensional flows. Therefore, rheological models such as Giesekus or PTT models (i.e, models having good performance in extensional flows) should be used in studies related to peristaltic flows.

In two recent works, peristaltic flow of Giesekus fluids has been investigated[10,11] in straight and curved channels. But, a rheological model known to have a better performance in extensional flows is the Phan-Thien-Tanner (PTT) model. To the best of our knowledge, there is no published addressing peristaltic flow of PTT fluids in

the open literature. So, in the present work we have decided to rely on the PTT model to investigate viscoelastic effects on peristaltic flow[12]. To better simulate physiological systems encountered in human bodies, the flow passage is assumed to be curved[13,14]. We are particularly interested in knowing how the extensional parameter which appears in the PTT model affects peristaltic flows. To add to its generality, we are going to investigate the effect of a radially-imposed magnetic field on the flow characteristics. Our interest in magnetic field stems from the fact *magnetotherapy is increasingly* being used as an active means for therapy of certain diseases in medical science[15-17].

MATHEMATICAL FORMULATION

Figure 1 shows the curved channel of mean radius $\bar{R}$ and average height of $2a_0$. A wave with phase velocity c, wavelength λ_c, and amplitude a_1 is seen to be propagating from right to left along the upper and lower walls of the channel. The waves are taken to be of the following form:

$$R(X,t)_{Outer} = a_0 + a_1 \sin\left(\frac{2\pi}{\lambda_c}(X-ct)\right), \tag{1a}$$

$$R(X,t)_{Inner} = -a_0 - a_1 \sin\left(\frac{2\pi}{\lambda_c}(X-ct)\right), \tag{1b}$$

where t is the time, X is the azimuthal coordinate, and R is the radial distance in a curvilinear coordinate system with its origin located at the mid-point of the channel (as shown in Fig. 1). The propagating wave forces the fluid to flow from right to left with U(R,X,t) and V(R,X,t) denoting velocity components in the azimuthal and radial directions, respectively. In addition to the peristaltic motion of the walls, the channel is seen to be simultaneously subjected to a magnetic field of strength B in the radial direction. We assume that the width of the channel perpendicular to the plane is infinite so that the flow can safely be taken as two-dimensional. We also assume that the fluid is incompressible. Since physiological systems normally involve low-Reynolds number flows, we can also assume that the flow is laminar.

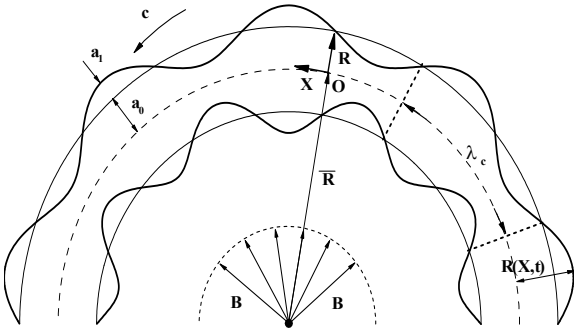

Figure 1. Schematic of peristaltic flow in a curved two-dimensional channel.

The equations governing flow induced in the channel are the continuity equation, and the Cauchy equations of motion, that is,

$$\nabla.\vec{\mathbf{V}} = 0, \tag{2a}$$

$$\rho\left(\frac{\partial\vec{\mathbf{V}}}{\partial t} + \left(\vec{\mathbf{V}}.\vec{\nabla}\right)\vec{\mathbf{V}}\right) = -\nabla p + \nabla.\underset{\sim}{\tau} + \vec{\mathbf{J}}\times\vec{\mathbf{B}}, \tag{2b}$$

where p is the isotropic pressure, τ is the stress tensor, ρ is the fluid's density, J is the current density, and B is the radial magnetic field.

For ease of analysis, we assume that the magnetic Reynolds number is very small so that the induced magnetic and electric fields (as generated by the motion of the electrically-conducting fluid) can be neglected[20]. From Maxwell equations and Ohm's law we obtain[20].

$$\vec{\mathbf{B}} = \left(\frac{B_0}{R+\bar{R}}\right)e_R \tag{3}$$

where B_0 is the characteristic magnetic induction, and e_R is the unit vector in the radial direction. The term J×B in Eq. 2b can be written as[39]:

$$\vec{\mathbf{J}}\times\vec{\mathbf{B}}=-\left(\frac{\sigma_e B_0^2}{\left(R+\bar{R}\right)^2}U\right)e_X. \tag{4}$$

where e_X is the unit vector in the azimuthal direction. We assume that the fluid of interest obeys the Phan-Thien-Tanner (PTT) model as its constitutive equation[12] . In its most general form, the model is written as:

$$\begin{aligned} &Z\left(\mathrm{tr}\,\underset{\sim}{\tau}\right)\underset{\sim}{\tau}+\lambda\left(\frac{\partial\underset{\sim}{\tau}}{\partial t}+\left(\vec{\mathbf{V}}.\vec{\nabla}\right)\underset{\sim}{\tau}-\left(\underset{\sim}{\tau}.\nabla\vec{\mathbf{V}}+\nabla\vec{\mathbf{V}}^{T}.\underset{\sim}{\tau}\right)\right)\\ &+\xi\lambda\left(\underset{\sim}{\tau}.\underset{\sim}{D}+\underset{\sim}{D}.\underset{\sim}{\tau}\right)=2\eta\underset{\sim}{D}\end{aligned} \tag{5}$$

where D is the rate of deformation tensor, η is the zero-shear viscosity, ξ is a parameter related to the slip between the molecular network, and λ is the relaxation time. The stress coefficient, $Z(\mathrm{tr}\,\underset{\sim}{\tau})$, is an exponential function of $\mathrm{tr}\,\underset{\sim}{\tau}$. At small deformation rates, it can be linearized to:

$$Z\left(\mathrm{tr}\,\underset{\sim}{\tau}\right)=1+\frac{\varepsilon\lambda}{\eta}\mathrm{tr}\,\underset{\sim}{\tau} \tag{6}$$

where ε is the elongational parameter of the model. This version of the model is easier to work with, and so it will be used in this work[20]. As to the boundary conditions required to close the problem, we are going to rely on the no-slip and no-penetration velocity boundary conditions at the non-compliant walls of the channel. The frame of reference can be changed to a wave-frame coordinate system such that the flow can be considered as steady. To that end, we set[1],

$$(x=X-ct,\ r=R)\ ,\ (u=U-c,\ v=V). \tag{7}$$

Also, to work with dimensionless parameters, we substitute:

$$\begin{aligned} &u^*=\frac{u}{c},\ v^*=\frac{v}{c\delta},\ x^*=\frac{2\pi x}{\lambda_c},\ r^*=\frac{r}{a_0},\\ &\tau^*=\frac{a_0}{c\eta}\tau,\ p^*=\frac{2\pi a_0^2}{\lambda_c\eta c}p,\ k=\frac{\bar{R}}{a_0},\ \varphi=\frac{a_1}{a_0}\end{aligned} \tag{8}$$

where k is the curvature parameter, φ is the amplitude ratio, and δ is the wavelength ratio defined by $\delta = 2\pi a_0/\lambda_c$. Having dropped "*" for convenience, the dimensionless forms of the governing equations become[18],

$$\frac{\partial}{\partial r}\{(r+k)v\}+k\frac{\partial u}{\partial x}=0 \tag{9a}$$

$$\begin{aligned} &\mathrm{Re}.\delta\left(-\delta^2\frac{\partial v}{\partial x}+\delta^2 v\frac{\partial v}{\partial r}+\delta^2\frac{k(u+1)}{r+k}\frac{\partial v}{\partial x}-\frac{(u+1)^2}{r+k}\right)\\ &=-\frac{\partial p}{\partial r}+\left(\frac{\delta}{r+k}\right)\frac{\partial}{\partial r}\{(r+k)\tau_{rr}\}+\\ &\delta^2\left(\frac{k}{r+k}\right)\frac{\partial\tau_{rx}}{\partial x}-\left(\frac{\delta}{r+k}\right)\tau_{xx}\end{aligned} \tag{9b}$$

$$\begin{aligned} &\mathrm{Re}.\delta\left(-\frac{\partial u}{\partial x}+v\frac{\partial u}{\partial r}+\frac{k(u+1)}{r+k}\frac{\partial u}{\partial x}+\frac{(u+1)v}{r+k}\right)\\ &=-\left(\frac{k}{r+k}\right)\frac{\partial p}{\partial x}+\frac{1}{(r+k)^2}\frac{\partial}{\partial r}\{(r+k)^2\tau_{rx}\}+\\ &\delta\left(\frac{k}{r+k}\right)\frac{\partial\tau_{xx}}{\partial x}-\mathrm{Ha}^2\frac{(u+1)}{(r+k)^2}\end{aligned} \tag{9c}$$

where $\mathrm{Re}=\rho c a_0/\eta$ is the Reynolds number, and $\mathrm{Ha}=B_0\sqrt{\sigma_e/\eta}$ is the Hartman number. To simplify the above equations, we rely on the long-wavelength assumption (i.e., $\delta\to 0$). In addition to this, we assume that the Reynolds number is vanishingly small. These assumptions are quite common in the context of peristaltic flows and are considered convenient for the purposes of this work[18]. On the basis of these assumptions, the equations of motion are reduced to[18]:

$$\frac{\partial p}{\partial r}\approx 0 \tag{10a}$$

$$-\frac{\partial p}{\partial x}+\frac{1}{k(r+k)}\frac{\partial}{\partial r}\left\{(r+k)^2\tau_{rx}\right\}-\mathrm{Ha}^2\frac{1-\frac{\partial\psi}{\partial r}}{k(r+k)}=0 \tag{10b}$$

where ψ is the stream function defined by:

$$u = -\frac{\partial \psi}{\partial r}, \quad v = \frac{k}{r+k}\frac{\partial \psi}{\partial x}. \tag{11}$$

It is also easy to show that the simplified form of the stress terms are[18]:

$$\left(1+\varepsilon We\left(\tau_{rr}+\tau_{xx}\right)\right)\tau_{rr} = -\xi We\dot{\gamma}\tau_{rx} \tag{12a}$$

$$\left(1+\varepsilon We\left(\tau_{rr}+\tau_{xx}\right)\right)\tau_{rx} = \dot{\gamma} + We\left(1-\frac{\xi}{2}\right)\dot{\gamma}\tau_{rr} - \frac{\xi We}{2}\dot{\gamma}\tau_{xx} \tag{12b}$$

$$\left(1+\varepsilon We\left(\tau_{rr}+\tau_{xx}\right)\right)\tau_{xx} = We\left(2-\xi\right)\dot{\gamma}\tau_{rx} \tag{12c}$$

where We = $\lambda c/a_0$ is the Weissenberg number and $\dot{\gamma}$ is the shear rate defined by[18]:

$$\dot{\gamma} = (r+k)\frac{\partial}{\partial r}\left((1-\frac{\partial \psi}{\partial r})\Big/(r+k)\right). \tag{13}$$

The ratio of Eqs. 12a and 12c leads to the relation between the normal stresses:

$$\frac{\tau_{rr}}{\tau_{xx}} = -\frac{\xi}{2-\xi} \tag{14}$$

By dividing Eq. 12b by Eq. 12c and substituting τ_{rr} from Eq. 14, the following equation is obtained for τ_{xx} :

$$\tau_{xx} = \frac{1 \pm \sqrt{1-4\xi\left(2-\xi\right)We^2\tau_{rx}^2}}{2\xi We}, \tag{15}$$

where we have discarded the other root so that τ_{xx} remains finite when ξ approaches zero. The shear rate $\dot{\gamma}$ can be obtained as a function of shear stress by substituting τ_{xx} from Eq. 15 into Eq. 12c:

$$\dot{\gamma} = \frac{\left(1-\sqrt{1-4\xi\left(2-\xi\right)We^2\tau_{rx}^2}\right)}{2\xi\left(2-\xi\right)We^2\tau_{rx}} \times \left\{1+\frac{\varepsilon(1-\xi)}{\xi(2-\xi)}\left(1-\sqrt{1-4\xi\left(2-\xi\right)We^2\tau_{rx}^2}\right)\right\} \tag{16}$$

when ξ approaches to zero, the constitutive Eq. 5 reduces to simplified PTT fluid. For such a case, the stress components are represented by:

$$\tau_{xx} = 2We\tau_{rx}^2, \tau_{rr} = 0 \tag{17a}$$

$$\dot{\gamma} = \left(1+2\varepsilon We^2\tau_{rx}^2\right)\tau_{rx} \tag{17b}$$

Having obtained the velocity components, we can obtain dp/dx from Eq. 10b for one wavelength. Similarly, we can obtain the flow rate as,

$$Q = q + 2 \tag{18}$$

where Q and q are the flow rate in the original and wave-frame coordinate systems, respectively.

NUMERICAL METHOD OF SOLUTION

By eliminating the pressure between Eq. 10a and Eq. 10b, the equation of motion is obtained as[18]:

$$\frac{\left(r+k\right)}{3}\frac{\partial^2\tau_{rx}}{\partial r^2} + \frac{\partial \tau_{rx}}{\partial r} + \frac{Ha^2}{3\left(r+k\right)}\left(\frac{\partial^2\psi}{\partial r^2} + \frac{1}{r+k}\left(1-\frac{\partial \psi}{\partial r}\right)\right) = 0 \tag{19a}$$

Substituting Eq.13 into Eq. 16, we will then end up with[39]:

$$-\frac{\partial^2\psi}{\partial r^2} - \frac{1}{r+k}\left(1-\frac{\partial \psi}{\partial r}\right) = \frac{\left(1-\sqrt{1-4\xi\left(2-\xi\right)We^2\tau_{rx}^2}\right)}{2\xi\left(2-\xi\right)We^2\tau_{rx}} \times \left\{1+\frac{\varepsilon(1-\xi)}{\xi(2-\xi)}\left(1-\sqrt{1-4\xi\left(2-\xi\right)We^2\tau_{rx}^2}\right)\right\} \tag{19b}$$

Equations 19a,b cannot be reduced into a single ODE because stress terms in the PTT model are implicitly related to the velocity field, rather than explicitly. Indeed, these two equations form a nonlinear system of ODEs that should be solved simultaneously

subject to the following boundary conditions[18]:

$$\text{at } r(x)_{\text{Outer}} = 1+\varphi\sin(x): \frac{\partial\psi}{\partial r} = 1,\ \psi = -\frac{q}{2} \quad (20a)$$

$$\text{at } r(x)_{\text{Inner}} = -1-\varphi\sin(x): \frac{\partial\psi}{\partial r} = 1,\ \psi = +\frac{q}{2} \quad (20b)$$

By eliminating the stream function between Eq. 19a and Eq. 19b, the differential equation for the shear stress, τ_{rx}, is obtained as[18]:

$$\frac{(r+k)}{3}\frac{\partial^2\tau_{rx}}{\partial r^2}+\frac{\partial\tau_{rx}}{\partial r} = \left(1-\sqrt{1-4\xi(2-\xi)We^2\tau_{rx}^2}\right) \times \frac{M^2\left\{1+\frac{\varepsilon(1-\xi)}{\xi(2-\xi)}\left(1-\sqrt{1-4\xi(2-\xi)We^2\tau_{rx}^2}\right)\right\}}{6\xi(2-\xi)We^2(r+k)\tau_{rx}} \quad (21)$$

We have relied on the Finite Difference Method (FDM) for solving this system of equations using a shooting scheme. That is: first, we guess the shear stress at inner and outer walls of the channel starting from Newtonian values. From Eq. 21 we then obtain the distribution of the shear stress, τ_{rx}, across the channel for the first iteration. Having obtained τ_{rx}, we can then proceed with calculating the stream function ψ from Eqs. 19a,b for any given set of Ha, We, ε, and ξ using the two known boundary conditions from Eq. 20b. The accuracy of the initial guess is checked by calculating the two left boundary conditions and comparing them with those in Eq. 20a. This procedure is repeated until the two left boundary conditions are satisfied within a tolerance of 10^{-6}.

It is worth-mentioning that in our FDM formulations, all derivatives are calculated using the second-order central differencing scheme.

RESULTS AND DISCUSSIONS

Having verified the code using Newtonian results in straight channels, the code was used to investigate the effect of different parameters on flow characteristics. We are going to present typical results only[18]. To that end, we fix the amplitude ratio at $\varphi = 0.4$ and slip factor at $\xi = 0.01$.

Figures 2 and 3 show the effect of Weissenberg number and also the extensional parameter on the azimuthal velocity profile at $x = -\pi/2$ location for $Q = 1,\ k = 3,$ and $Ha = 0.$ As can be seen in these figures, by an increase in the Weissenberg number and/or the extensional parameter, the velocity is decreased near the channel centreline while it is slightly increased near the channel walls. This is not surprising realizing the fact that viscoelastic fluids are generally strain-hardening. That is to say that, their extensional viscosity increases by an increase in the extension rate. The rate of extension is obviously largest at the channel's centreline, and so a drop in velocity at the centreline is as expected. On the other hand, an increase in the velocity near the wall can be attributed to the shear-thinning behaviour of PTT fluids. The shear-thinning is more significant near the wall region (i.e., where the shear rate is the largest) and this can more than counterbalance the retarding effect of the extensional viscosity of the fluid which is quite small near the wall.

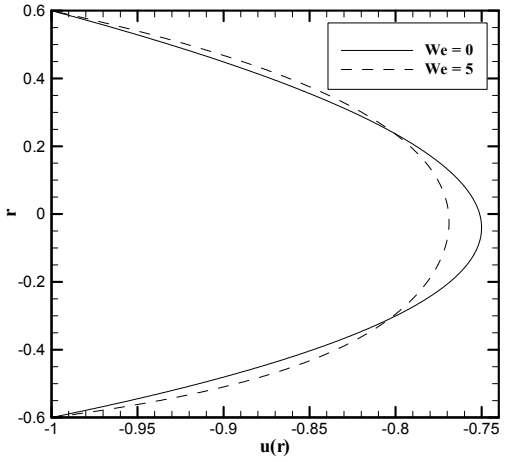

Figure 2. Effect of Weissenberg number on the azimuthal velocity profile obtained at $\varepsilon = 0.1,$ and $\xi = 0.01$.

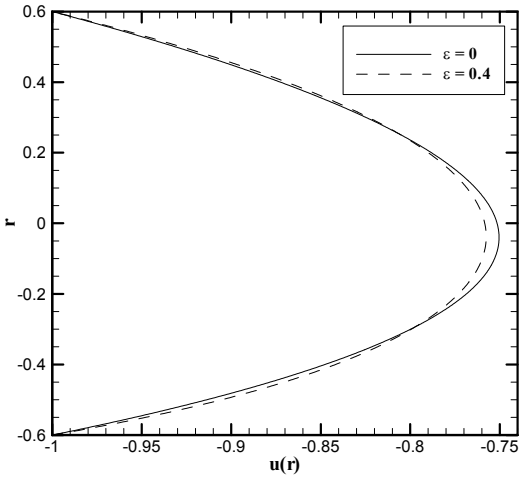

Figure 3. Effect of the extensional parameter on the azimuthal velocity obtained at ($We = 1,\ \xi = 0.01$)

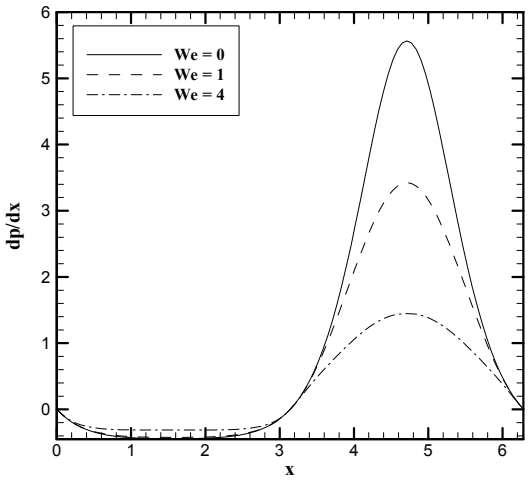

Figure 4. Effect of Weissenberg number on the peristaltic pressure gradient ($\varepsilon = 0.1,\ \xi = 0.01$)

Knowing the velocity and stress fields, one can proceed with calculating the pressure gradient term, dp/dx, from Eq. 10b. Figures 4 and 5 show the effect of Weissenberg number and the extensional parameter on the pressure gradient along the channel centerline for one wavelength obtained at $Q = 0, k = 5,$ and $Ha = 0$. The elastic behaviour of the fluid is seen to reduce the magnitude of the pressure gradient along the channel, and this is particularly so at $x = 3\pi/2$ (i.e., at location the channel height is minimum).

To interpret the numerical results shown in Figs. 4 and 5, it should be noted that the pressure gradient as generated by the peristaltic motion of the walls is closely related to the shear stress and azimuthal normal stress which are both controlled by fluid's elasticity (see Eq. 9c). Obviously, at the minimum area of the channel fluid elements are subjected to the largest deformation rates. This means that the extensional viscosity of the fluid is maximum at this location with a subsequent resisting effect on the flow effectively reducing the pressure gradient at this location (see Figs. 4 and 5).

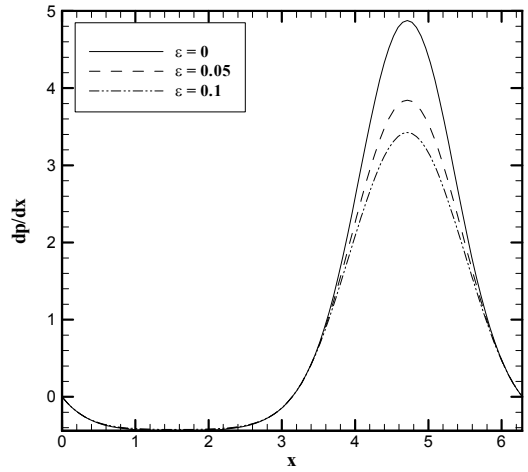

Figure 5. Effect of extensional parameter on the peristaltic pressure gradient ($We = 1,\ \xi = 0.01$)

Knowing the azimuthal pressure gradient, we can proceed with calculating the $\Delta p - Q$ profile. Figures 6 and 7 show the effect of the Weissenberg number and extensional parameter on the velocity profile obtained at $k = 5,$ and $Ha = 0$. Obviously, for the peristaltic motion of the walls to act as a pump, we should have $\Delta p > 0$. As can be seen in Figs. 6 and 7, this is true only over a limited range of flow rates. And, over this

range of flow rates, the elastic behaviour of a fluid is predicted to decrease the pressure rise of peristaltic pumps.

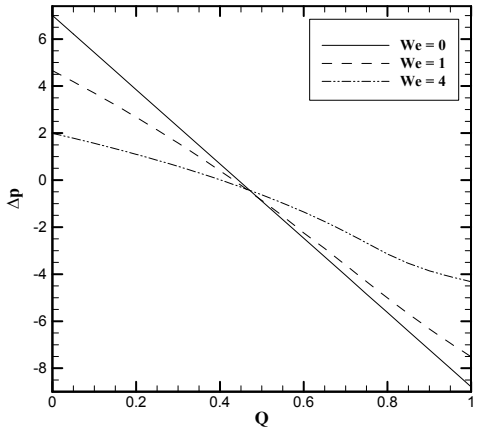

Figure 6. Effect of the Weissenberg number on the pressure rise of the pump
($\varepsilon = 0.1,\ \xi = 0.01$)

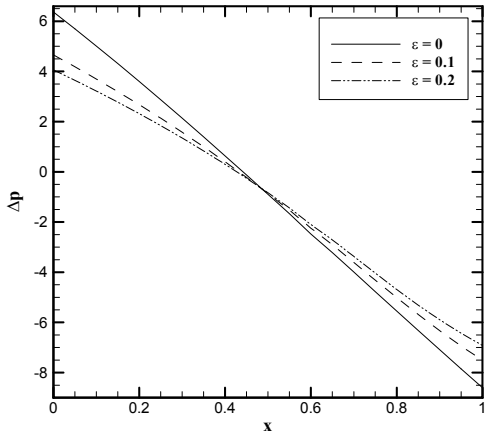

Figure 7. Effect of the extensional parameter on the pressure rise of the pump
($\mathrm{We} = 1,\ \xi = 0.01$)

The above results show that fluid properties play a key role in affecting peristaltic pumping of viscoelastic fluids. Unfortunately, one cannot manipulate the rheological properties of the working fluid in order to passively control the performance of peristaltic pumps. In cases when fluid properties cannot be tempered with, one might rely on applying an external magnetic field as an active means for this purpose. Figure 8 shows the suitability of this method in controlling the performance of peristaltic pumps obtained at $\mathrm{We} = 1, \varepsilon = 0.1, \xi = 0.01$.

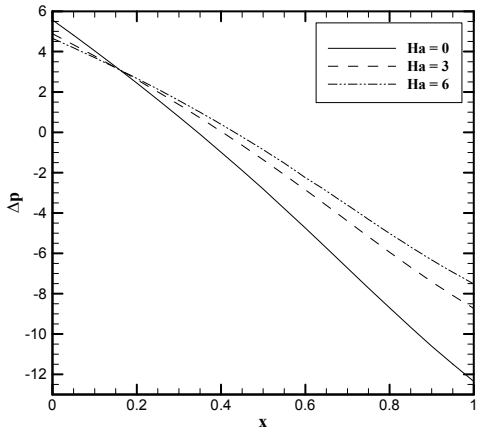

Figure 8. Effect of magnetic field on the pressure rise of peristaltic pump
($\mathrm{We} = 1,\ \varepsilon = 0.1,\ \xi = 0.01$)

CONCLUDING REMARKS

Based on the results obtained in the present work, one can conclude that in peristaltic flows of viscoelastic fluids, the elastic behaviour of the fluid can dramatically affect flow kinematics and dynamics even under creeping-flow conditions. Results show that at a given flow rate, the elastic behavior of the fluid (as represented by the Weissenberg number) causes a decrease in the pressure rise of the pump. The effect of the extensional parameter is shown to be qualitatively similar to the effect of the Weissenberg number. An externally-imposed magnetic field is found to be a powerful tool for controlling the pumping effect of the geometry provided that the flow rate is less than a critical value.

ACKNOWLEDGEMENT

The authors would like to thank Center of Excellence in Design and Optimization of Energy Systems (CEDOES): University of Tehran, Department of Mechanical Engineering, for supporting this work.

REFERENCES

1. Latham, T.W. (1966), "Fluid motion in peristaltic pump", MS thesis, MIII, Cambridge, Mass.

2. Burns, J.C. and Pareks, J. (1967), "Peristaltic motion", *J. Fluid Mech*., **29** 731–43.

3. Reddy, M.V.S., Rao, A.R., and Sreenadh, S. (2007), "Peristaltic motion of a power-law fluid in an asymmetric channel", *Int. J. Nonlinear Mech.,* **42**, 1153-1161.

4. Böhme, G. and Friedrich, R. (1983), "Peristaltic flow of viscoelastic liquids", *J. Fluid Mech.,* **128**, 109-122.

5. Siddiqui, A.M., Provost, A., and Schwarz, W. H. (1994), "Peristaltic flow of a second order fluid in tubes", *J. Non-Newtonian Fluid Mech.,* **53**, 257-284.

6. Hayat, T., Wang, Y., Siddiqui, A.M., Hutter, K., and Asghar, S. (2002), "Peristaltic transport of a third-order fluid in a circular cylindrical tube", *Math. Models and Methods in Appl. Sci.,* **12**, 1691-1706.

7. Haroun, M.H. (2007), "Non-linear peristaltic flow of a fourth-grade fluid in an inclined asymmetric channel*", Compu. Mat. Sci.,* **39**, 324-333.

8. Hayat, T., Wang, Y., Hutter, K., Asghar, S., and Siddiqui, A.M. (2004), "Peristaltic transport of an Oldroyd-B fluid in a planar channel", Math. Problems. Eng., **4**, 347-376.

9. Hayat, T., Wang, Y., Siddiqui, A. M., and Hutter, K. (2003), "Peristaltic motion of Johnson-Segalman fluid in a planar channel", *Math. Problems. Eng.,* **1**, 1-23.

10. Nasir A., Tariq J., Flow of Giesekus fluid in a planar channel due to peristalsis, submitted for publication, *Z. Naturforsch*, 2013.

11. Kalantari A., Riasi A. Sadeghy K., Peristaltic Flow of Giesekus Fluids through Curved Channels: an Approximate Solution, accepted for publication, *J. Society of Rheology: Japan*, 2013.

12. Bird R.B., Armstrong R.C., and Hassager O., (1987), "Dynamics of Polymeric Liquids", second ed., vol. 1, John Wiley& Sons, New York.

13. Sato, H., Kawai, T., Fujita, T., and Okabe, M. (2000), "Two dimensional peristaltic flow in curved channels", *Trans. The Japan Soc. Mech. Eng.,* B **66**, 679-685.

14. Ali, N., Sajid, M., Abbas, Z., and Javed, T. (2010), "Non-Newtonian fluid flow induced by peristaltic waves in a curved channel", *Eur. J. Mech. B/Fluids,* **29** 3511–3521.

15. Mekheimer, Kh.S. (2004), "Peristaltic flow of blood under effect of a magnetic field in a nonuniform channels", *Appl Math Comput,* **153**, 763-777.

16. Hakeem, A.E., Naby, A.E., El Misery, MF, and Kareem, A.E.M. (2006), "Effects of magnetic field on trapping through peristaltic motion for generalized Newtonian fluid in channel", Physica A, **367**, 79-92.

17. Hayat, T., Noreen, S., and Alsaedi, A. (2012), "Effect of an induced magnetic field on peristaltic flow of non-Newtonian fluid in a curved channel", *Journal of Mechanics in Medicine and Biology,* **12**, No. 3, 1250058 (26 pages).

18. Kalantari, A. (2012), "Peristaltic Flow of Viscoelastic Fluids through Curved Channels: a Numerical Study", M.Sc thesis, University of Tehran, 2012.